

Analyzing and Reducing Catastrophic Forgetting in Parameter Efficient Tuning

Weijieying Ren¹ Xinlong Li² Lei Wang³ Tianxiang Zhao¹ Wei Qin²

¹ College of Information Sciences and Technology, Pennsylvania State University

² School of Computer Science and Technology, Singapore Management University

³ School of Computer Science, Hefei Univeristy of Technology

{wjr5337, tkz5084}@psu.edu, lei.wang.2019@phdcs.smu.edu.sg,
qinwei.hfut@gmail.com

Abstract

Existing research has shown that large language models (LLMs) exhibit remarkable performance in language understanding and generation. However, when LLMs are continuously fine-tuned on complex and diverse domain-specific downstream tasks, the inference performance on historical tasks decreases dramatically, which is known as a catastrophic forgetting problem. A trade-off needs to be kept between learning plasticity and memory stability. Plenty of existing works have explored strategies like memory replay, regularization and parameter isolation, but little is known about the geometric connection of various adjacent minima in the continual LLMs fine-tuning scenarios. In this work, we investigate the geometric connections of different minima through the lens of mode connectivity, which means different minima can be connected by a low-loss valley. Through extensive experiments, we uncover the mode connectivity phenomenon in the LLMs continual learning scenario and find that it can strike a balance between plasticity and stability. Building upon these findings, we propose a simple yet effective method called Interpolation-based LoRA (I-LoRA), which constructs a dual-memory experience replay framework based on LoRA parameter interpolations. Extensive experiments and analysis on eight domain-specific CL benchmarks demonstrate that I-LoRA consistently show significant improvement over the previous state-of-the-art approaches with up to 11% performance gains, providing a strong baseline and insights for future research on the large language model continual learning problem. Our code is available at <https://github.com/which47/LLMCL>.

1 Introduction

Despite the impressive zero-shot and few-shot learning capabilities demonstrated by generative Large Language Models (LLMs) (Wang et al., 2023a), their performance degrades largely in the

continual learning (CL) scenario, which requires the adaptation to complex new tasks while preserving previously learned knowledge (Razdaibiedina et al., 2023). This problem is known as catastrophic forgetting (Li and Hoiem, 2017), highlighted by the trade-off between learning plasticity (fast adaptation to novel tasks) and memory stability (preservation of learned knowledge).

Previous works have explored three directions to achieve a balance between plasticity and stability (Wang et al., 2023a). Among them, replay-based methods preserve historical information by explicitly storing a subset of historical data (Chaudhry et al., 2019b) or prompts (Khan et al., 2023). Regularization-based methods (Li and Hoiem, 2017) propose to penalize change of important model parameters or conduct embedding-level distillation from the historical model during the learning of new tasks. The third category, parameter isolation methods (Kang et al., 2022), mitigates forgetting by explicitly encoding task-specific model parameters, e.g., introducing a list of adapters to consolidate historical knowledge.

Despite these explorations, we argue that the essence of achieving plasticity-stability trade-off lies in the intersection of loss landscapes surrounding optima for various tasks (see Figure 4). Once the model has converged to the optima of historical tasks, there would be a region around it that achieves optimal performance for the new task. Moreover, there exists a parametric path connecting the optima of historical tasks to that of the new task, and a well-balanced trade-off can be attained by traversing model parameters along this path. This phenomenon is named “mode connectivity” (Garipov et al., 2018; Doan et al., 2023). Similar observations are made in the computer vision domain, which unifies CL with multi-task learning (Mirzadeh et al., 2020) and conducts class incremental learning (Wen et al., 2023). However, whether analogous observations hold in the LLM

domain remains an unexplored task. LLMs often involve intricate pre-training on large-scale corpora, dealing with nuanced contextual understanding and text generation. Analyzing the mode connectivity phenomenon holds seamlessly to LLMs is crucial for facilitating continual learning on them.

In this paper, we are the first to present such a new perspective in understanding and improving CL for Large Language Models. Specifically, we focus on the following research questions in the context of Parameter-Efficient Fine-Tuning (PEFT) strategies: **RQ1**: *Does mode connectivity exist for continual learning in PEFT?* and **RQ2**: *How can we leverage the geometric connections of different minima to address catastrophic forgetting in PEFT?* Based on experiments conducted across eight diverse and domain-specific CL benchmarks, our analysis reveals the following findings: 1) mode connectivity exists in the continual fine-tuning scenario of LLMs; 2) mode connectivity can be established by constructing a parametric path to connect historical and current optima; and 3) a more optimal trade-off between stability and plasticity can be achieved along a linear trajectory between the two optima. Based on these observations, we propose I-LoRA (Interpolation-based LoRA), which aims to simulate the weight interpolation process along with continual updates of LLMs using LoRA. Specifically, I-LoRA establishes a dual-memory framework by maintaining a fast learner parameterized by the working memory and a slow learner parameterized by the long-term memory. The fast learner is responsible for quick adapting to the evolving data, while the slow learner aims to consolidate the long-term memory and preserve historical knowledge. We iteratively update these two learners to achieve a balance between plasticity and stability.

The main contributions of this paper are listed as follows:

- We are the first to present a novel perspective on understanding the continual learning for LLMs on mode connectivity;
- Base on comprehensive analysis, we propose an effective CL algorithm for LLM by designing a dual-memory framework, with a fast learner to quickly adapt to evolving tasks and a slow learner to reduce forgetting;
- Extensive experiments and analysis of I-LoRA are conducted across diverse textual datasets,

which validate its strong performance in the trade-off between plasticity and stability.

2 Related Works

Continual Learning focuses on sequential learning of non-stationary data, ideally accumulating previously gained knowledge (Wang et al., 2023a). Based on the taxonomy in (Li and Hoiem, 2017), existing works can be broadly classified into three dimensions: 1) Replay-based methodologies involve the reloading of historical raw data (Rolnick et al., 2019; Buzzega et al., 2020) or the utilization of synthetic data (Lesort et al., 2019) generated from a generative model trained on historical data. 2) Regularization-based methods (Kirkpatrick et al., 2017; Saha et al., 2021; Kim et al., 2023) penalize model parameter change and balance the trade-off between plasticity and stability; 3) Parameter isolation methods (Kang et al., 2022; Golkar et al., 2019) identify, allocate and incorporate critical parameters for different tasks during CL, thereby minimizing the interaction between tasks. For an in-depth discussion on continual learning in the era of large language models, readers may refer to (Wang et al., 2023a).

Linear Mode Connectivity is a phenomenon that different minima can be connected by low-loss paths in the parameter space (Garipov et al., 2018; Entezari et al., 2021). Optimizing neural networks involves the finding of a minimum within a high-dimensional, non-convex objective landscape. (Frankle et al., 2020) asserts that, from the same initialization, local minima obtained with different training data orders can be interconnected by a linear low-loss path, thereby alleviating the challenge of curve identification. Building upon this discovery, recent research by (Mirzadeh et al., 2020) observes that solutions in multitask and continual learning scenarios are connected by straightforward curves exhibiting low errors in weight space. This phenomenon, termed Linear Mode Connectivity, is empirically demonstrated to be a linear path when both multitask learning and continual learning share the same initialization weights. However, these aforementioned works typically study mode connectivity using non-pretrained models in the field of computer vision (Wen et al., 2023; Zhao et al., 2020), weight pruning analysis (Pellegrini and Biroli, 2022), loss landscape analysis (Frankle et al., 2020; Garipov et al., 2018), and etc.

Recently, (Qin et al., 2022) pioneered the explo-

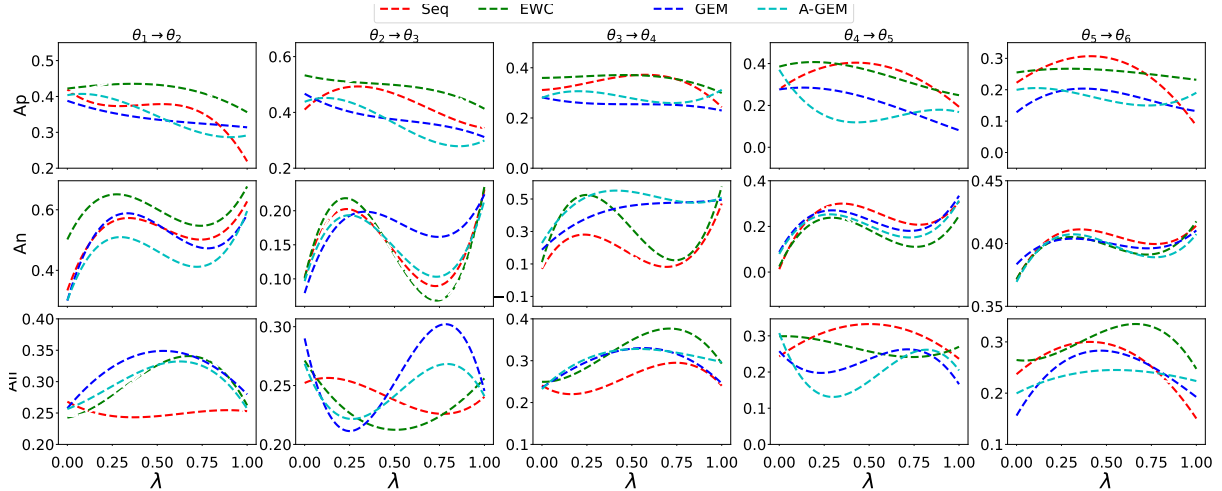


Figure 1: Inference accuracy curves along the linear connection between two adjacent continual minima of five representation continual learning baselines on seven domain-specific benchmarks. The y-axis, named Ap(upper row), An(mid row), and Aall(bottom row) denotes accuracy on previous tasks $1 : t$, on the current task $t + 1$, and on all learned tasks $1 : (t + 1)$ respectively. X-axis, λ indicates the interpolation factor. Taking the testing accuracy as the measure of connectivity is because it is more sensitive to moving along the path than training loss.

ration of mode connectivity analysis on pretrained models, revealing that although minima trained on different tasks are inherently disconnected, pre-training gradually brings the optimal regions of diverse tasks closer in an implicit manner. In this study, we are the first to delve into continual learning within the framework of PEFT.

3 Analyzing Linear Mode Connectivity in Parameter Efficient Continual Learning for LLMs

In this section, we design an empirical study to answer RQ1, whether mode connectivity exists for continual learning in PEFT. We first introduce the notations and formulate the continual learning task before going into empirical details.

CL can be formulated as learning from a sequentially ordered set of tasks $\{\mathcal{D}_1, \mathcal{D}_2, \dots, \mathcal{D}_T\}$, where each task is specified by input-label pairs. To be specific, the t -th task is specified by $\mathcal{D}_t = \{(\mathbf{x}_i, y_i)\}_{i=1}^{N_t}$, where N_t represents the number of training examples for the t -th task. Formally, the objective of CL is to learn a function $f : \mathbb{R}^d \rightarrow \mathbb{R}$ with parameters $\theta \in \mathbb{R}^d$ that minimizes the loss over the tasks:

$$\min_{\theta} \mathbb{E}_{t=1}^T [\mathbb{E}_{(x,y) \sim \mathcal{D}_t} [\ell(f_{\theta}(x), y)]], \quad (1)$$

where ℓ is the learning objective of target tasks, e.g., cross-entropy loss. In this study, we adopt one representative PEFT approach, LoRA, and the model f comprises a large amount of pre-trained

fixed parameters and a small number of tunable parameters (the LoRA module). For the simplicity of annotation, throughout this paper, we use θ to denote those tunable parameters.

3.1 Mode Connectivity Evaluation

Given the minima of two adjacent tasks, denoted as θ_t and θ_{t+1} , we posit the existence of a continuous curve $\phi(\lambda) : [0, 1] \rightarrow \mathbb{R}^d$ connecting these minima. This curve represents a trajectory in the parameter space that smoothly transits from θ_t to θ_{t+1} . The linear path connecting the two minima can be expressed as follows:

$$\phi(\lambda) = (1 - \lambda) \cdot \theta_t + \lambda \cdot \theta_{t+1}. \quad (2)$$

Essentially, traversing along the curve described in Equation 2 allows for the evaluation of the interpolation performance between stability (where $\phi(0) = \theta_t$) and plasticity (where $\phi(1) = \theta_{t+1}$). It is expected that a better trade-off would exist along this trajectory, and the two endpoints θ_{t-1} and θ_t are smoothly connected without significant loss barrier or performance drop along the path. The evaluation performance on historical tasks, current tasks, and all tasks are abbreviated as Ap, An, and All, respectively.

Empirical Observations We investigate the existence of mode connectivity in Pre-trained Language Models (PLMs) during the continual fine-tuning across multiple downstream tasks in Figure 1. For space limitation, we report the performance

on the first six tasks with the same task order in Table 1. The sequence of tasks and experimental setups are further introduced in the experiment section, and we adopt LoRA during the tuning. After continually learned for each task, we conduct linear interpolations (parameterized by λ) between initial parameters (previous optima) and current ones (optima of the current task), and evaluate model performances with different λ values.

From Figure 1, we obtain the following observations: (1) The evaluation performance on the previous task t (denoted as Ap) could be significantly enhanced along the linear trajectory $\theta_t \rightarrow \theta_{t+1}$ compared to the initial point. This result suggests that parameters obtained along this trajectory may replace θ_t to achieve better memorization effects. (2) There are points along the linear path $\theta_t \rightarrow \theta_{t+1}$ yielding superior performance w.r.t the averaged past and current tasks, implying that a better trade-off between stability and plasticity can be achieved along this linear interpolation than the end-points. (3) Moreover, there are even intervals along the linear path $\theta_t \rightarrow \theta_{t+1}$ that exhibit comparable or superior accuracy on the current task $t+1$ (denoted as An) when compared to both endpoints. This observation suggests that points sampled within such intervals may serve as a better checkpoint for the current task $t+1$, surpassing the efficacy of θ_{t+1} .

4 Methodology

Inspired by the existence of ‘‘mode connectivity’’, we propose a simple yet effective method, Interpolation-based LoRA (I-LoRA), to keep the balance between rapid adaptation and knowledge preservation in the PEFT process. I-LoRA constructs a dual-memory experience replay framework by maintaining a long-term memory θ^l for stability and a working memory θ^w for plasticity and improves the trade-off with the idea of interpolation across optima. Next, we will introduce the design of dual memory in Section 4.1 before presenting the full algorithm in Section 4.2.

4.1 Dual Memory for Fast and Slow Learning

In this work, we adopt a *dual-memory* architecture to facilitate the separate encoding of historical and new optima, which enables us to explicitly estimate the trade-off. The framework comprises a fast learner (parameterized by working memory θ^w) and a slow learner (parameterized by long-term memory θ^l). The working memory, θ^w , is

learned by simulating the fast learning of each new task. For task t , at each step k , it will be optimized on back-propagated gradients from modeling $\mathcal{D}_t = \{(\mathbf{x}_i, y_i)\}_{i=1}^{N_t}$. θ^w can be understood as learning to arrive at the optima of this new task, converging to θ_{t+1}^* .

To keep the balance between historical and new knowledge, we further leverage a long-term memory, denoted as θ^l . As observed in Section 3.1, a better trade-off can often be discovered along the path connecting the optima θ_{t-1}^* and θ_t^* . However, it is challenging and computationally extensive to explicitly identify the optimal λ in Equation 2. To mitigate this problem, we conduct an iterative update of θ^l as an exponential moving average of the fast learner weights θ^w along the trajectory:

$$\theta_k^l = \lambda \cdot \theta_{k-1}^l + (1 - \lambda) \cdot \theta_k^w, \quad (3)$$

in which the step size λ is a fixed hyper-parameter and k denotes the update step. At each step, the previously learned θ_{k-1}^l will also modulate the obtention of θ_{k-1}^l to encourage a data-driven tuning of memorization effect, the detail of which will be introduced next.

Algorithm 1: I-LoRA

```

1 Input data stream  $\mathcal{D}$ , memory  $\mathcal{M}$ , Learning rate  $\eta$ ,
  update frequency  $a$ , update ratio  $\lambda$ 
2 for  $t \in [1, 2, \dots, T]$  do
3   for  $k$  in Training steps do
4     Sampling  $(\mathbf{x}, y) \in \mathcal{D}_t \cup \mathcal{M}$ 
5      $\mathcal{L}_{CE} \leftarrow \text{cross-entropy}(f(\mathbf{x}; \theta^w), y)$ 
6     Sampling  $(\mathbf{x}_m, y_m) \in \mathcal{M}$ 
7      $\mathbf{z}_m \leftarrow f_o(\mathbf{x}_m; \theta_k^l)$ 
8      $\mathcal{L}_{MSE} \leftarrow \text{mean-square}(f_o(\mathbf{x}_m; \theta^w), \mathbf{z}_m)$ 
9      $\mathcal{L} = \mathcal{L}_{CE} + \gamma \cdot \mathcal{L}_{MSE}$ 
10     $\theta_k^w \leftarrow \theta_{k-1}^w - \eta \nabla_{\theta_{k-1}^w} \mathcal{L}$ 
11     $\theta_k^l \leftarrow \lambda \theta_{k-1}^l + (1 - \lambda) \theta_k^w$ 
12  end
13   $\mathcal{M} \leftarrow \{\mathbf{x}_t, y_t\} \cup \mathcal{M}$ 
14 end

```

4.2 Continual PEFT with Dual Memory

Now we present details of the proposed continual PEFT algorithm, which is summarized in Algorithm 1. Both the working memory θ^w and long-term memory θ^l are implemented as LoRA modules. And we adopt the classical experience replay (ER) as our backbone framework: a subset of historical data is kept in an external episodic storage $\mathbf{x}_m \in \mathcal{M}$, which will be mixed with the current dataset $\mathbf{x}_t \in \mathcal{D}_t$ during learning.

For task t , during each training step, we optimize the fast learner (parameterized by θ^w) using (1) the

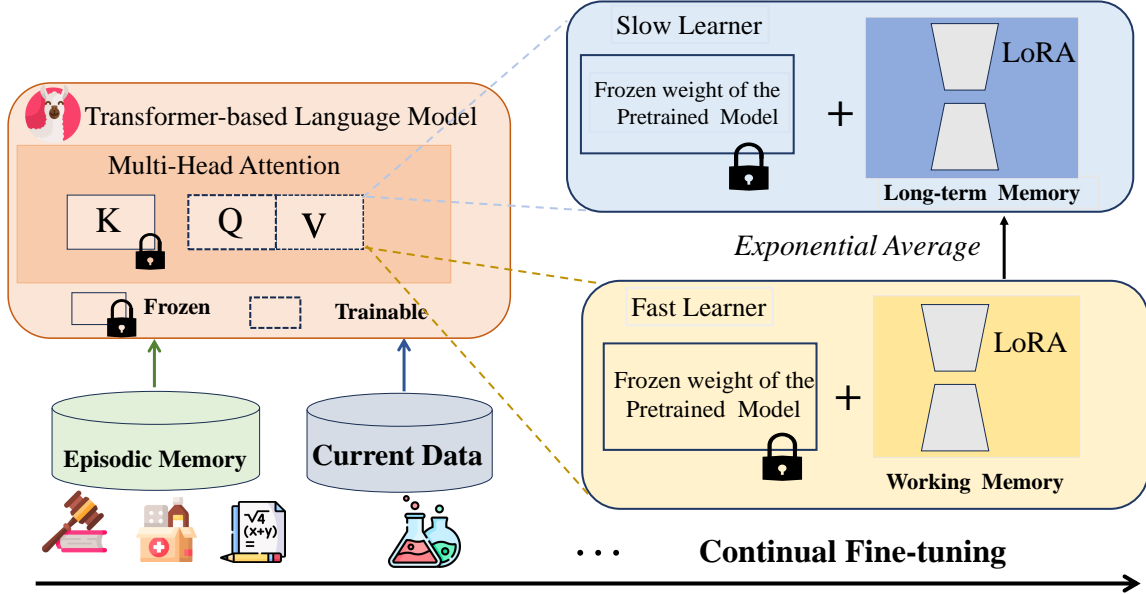


Figure 2: The framework of I-LoRA for Large Language Model Continual Learning. I-LoRA consists of a slow learner (depicted in blue) that learn long-term knowledge through exponential moving average of the fast learner weights; and (ii) a fast learner (depicted in yellow) retrieves historical knowledge while simultaneously adapting to current data. Both learners can be trained synchronously.

classification objective, as in line 5 of Algorithm 1, and (2) the deviation of historical instance embeddings compared to the slow learner (parameterized by θ^l), as in line 8. The former objective is implemented as a cross-entropy loss on the mixed data $\mathcal{M} \cup \mathcal{D}_t$, while the latter objective is implemented as the MSE loss on embeddings:

$$\begin{aligned} \min_{\theta^w} \mathcal{L} = & \mathbb{E}_{\mathbf{x} \in \mathcal{M} \cup \mathcal{D}_t} \mathcal{L}_{CE}(f(\mathbf{x}; \theta^w)) \\ & + \gamma \cdot \mathbb{E}_{\mathbf{x} \in \mathcal{M}} \mathcal{L}_{MSE}(f_o(\mathbf{x}; \theta^w); \mathbf{z}), \end{aligned} \quad (4)$$

where we omit task index t for simplicity. In this equation, f_o denotes the embedding extractor part of f , which maps the input into a representation space. \mathbf{z} records the embeddings generated by the slow learner, $f_o(\mathbf{x}; \theta^w)$ represents the output of the fast learner, and γ is a hyper-parameter controlling the weight of embedding deviation loss. An update of θ^w is provided in Line 10 of Algorithm 1. After each step, the slow learner will be updated as an exponential moving average of the fast learner weights, as in line 11.

5 Experiments

5.1 Experiment Setup

5.1.1 Dataset Description

To undertake a critical assessment of the ‘adaptation’ and ‘forgetting’ capabilities of LLMs (Wang

et al., 2023b; Gao et al., 2023), we construct the dataset under three key considerations: (I) *Domain Specificity*, avoiding prior exposure to the majority of LLMs; (II) *Diversity*, the dataset should be diverse and complex w.r.t corpus format, linguistic aspects, and reasoning challenges; (III) *Common sense knowledge*. In realistic scenarios, we aim to maintain the common sense knowledge in LLMs even when continually fine-tuning on diverse downstream tasks. To achieve such goals, we organize two types of datasets:

CL benchmarks for LLMs is to satisfy goal (I) and (II). Specifically, we organize datasets to demonstrate the following properties: 1) *Domain Specificity*. Continual training on diverse downstream tasks signifies a realistic and promising avenue for advancing LLMs. We select dataset from education domain, i.e., ScienceQA (Lu et al., 2022), clinical domain i.e., MedMCQA (Pal et al., 2022), financial domain, i.e., FOMC (Shah et al., 2023), legal domain, i.e., JEC-QA (Zhong et al., 2020), and political domain. i.e., MeetingBank (Hu et al., 2023). 2) *Multilinguality*. Cross-lingual Continual Learning poses a formidable challenge for LLMs attributed to vocabulary discrepancies and variations in pre-training corpus. Following (Wang et al., 2023b), We select C-STANCE (Zhao et al., 2023) and 20Minuten (Kew et al., 2023) as multi-lingual

dataset. 3) *Mathematical reasoning*. Mathematical problems involve complex logical operations, providing a test-bed for the reasoning ability of LLMs. Here, we leverage the popular NumGLUE dataset (Mishra et al., 2022).

General benchmarks for LLMs is to satisfy goal (III). We adopt MMLU (Hendrycks et al., 2021), BBH (Suzgun et al., 2022), and PIQA (Bisk et al., 2019) as our benchmark. A detailed description can refer to Appendix.

5.1.2 Metric

Let $R_{i,j}$ represents the inference accuracy on j -th task after training on the i -th, we evaluated the inference performance by averaging accuracy after the training of on the t -th task as Acc_t :

$$Acc_t = \frac{1}{T} \sum_{i=1}^t R_{t,i}. \quad (5)$$

Besides, we evaluate the memorization ability by evaluating the backward transfer ability (*BWT*) that averages influence of learning the t -th task on all old tasks as BWT_t (Wang et al., 2023a):

$$BWT_t = \frac{1}{t-1} \sum_{j=1}^{t-1} (R_{t,j} - R_{j,j}). \quad (6)$$

where T is the total number of data sequences.

5.1.3 Baselines

We evaluate the performance of I-LoRA against nine representative baseline methods. All baselines adopt the same architecture with LoRA for efficient fine-tuning. We maintain consistent parameter configurations across both I-LoRA and its comparative methods, thereby ensuring a fair comparison. We use the following baselines: (1) Zero-shot inference (ZSI): zero-shot inference on sequential downstream tasks directly without tuning model parameters or adding prompts. (2) Sequence Fine-tuning (Seq-Train): continual tuning all model parameters on a sequence of tasks (without adding any regularization or replaying samples from the previous tasks). (3) Experience Replay (ER) (Chaudhry et al., 2019b) typically stores a few old training samples within a small memory buffer. (4) Elastic Weight Consolidation (EWC) (Kirkpatrick et al., 2017) constrains important parameters to stay close to their old values and leverages the Fisher information matrix to measure the distance. (5) Gradient Gradient Episode Memory (GEM) (Saha et al., 2021): maintains the gradient

subspace important to the old tasks (i.e., the bases of core gradient space) for orthogonal projection in updating parameters. (6) Average Gradient Episode Memory (A-GEM) (Chaudhry et al., 2019a): a simple version of GEM that only stores the average gradient matrix on historical data. (7) Learning to Prompt (L2P) (Wang et al., 2022): uses the input to dynamically select and update prompts from the prompt pool in an instance-wise fashion. (8) Progressive Prompt (PP) (Razdaibiedina et al., 2023): learns a new soft prompt for each task and sequentially concatenates it with the previously learned prompts, while keeping the base model frozen. (9) Multi-task Learning (MTL): train a model on all tasks as multi-task learning. This method is assumed as the upper bound of continual learning (Wang et al., 2023a).

5.1.4 Implementation Details

Experiments are conducted on two RTX 4090 GPUs. We adopt Llama-2-7B as the foundational model and fine-tune LoRA (Hu et al., 2021) for continual learning purposes. The learning rate is set as $1e-4$, accompanied by a linear warmup ratio of 0.2. Following (Wang et al., 2023b), we leverage the HuggingFace Transformers (Wolf et al., 2020) library for experiment implementation. Regarding the LoRA hyper-parameters, r is set to 8, and LoRA is integrated into the query and value matrices, with the LoRA alpha parameter configured to 16.

For each dataset, we curate a training set comprising 5000 samples and an evaluation set comprising 500 samples. Batch-size is set as 16. Notably, in the case of MedMCQA and JEC-QA, our sampling process exclusively focuses on single-choice questions. Detailed demonstrates about prompts are shown in Table 4 in the Appendix.

5.2 Overall Comparison in CL

We first conducted a comparative analysis of our approach against representative CL baselines from two dimensions. First, we assessed the adaptation and memorization capabilities during continual learning on domain-specific CL benchmarks. Second, we evaluated the memorization ability of general knowledge when continually fine-tuning on domain-specific CL benchmarks.

Generalization Ability Assessment on Domain-specific CL benchmarks. We start with a fine-tuned LLaMA-7B language model on each domain-specific CL benchmark, then test the Acc_t performance to evaluate the adaptation

Domain-specific CL benchmarks for LLMs								
	C-STANCE	FOMC	MeetingBank	ScienceQA	NumGLUE-cm	20Minuten	MedMCQA	JEC-QA
Seq-Train	41.8	41.1	31.2	27.4	21.9	13.6	25.6	21.0
ER	40.8	45.6	30.6	29.4	18.7	16.5	22.8	22.4
EWC	42.2	53.0	35.9	38.5	25.5	26.2	23.5	22.5
GEM	38.8	46.4	28.3	27.4	12.7	17.7	28.5	20.4
A-GEM	40.2	43.9	28.0	36.9	19.8	22.6	27.3	29.6
L2P	43.8	39.5	24.0	26.4	22.7	15.4	24.6	25.6
PP	37.2	42.1	26.5	28.3	25.3	25.9	26.2	21.1
I-LoRA	44.4	53.9	30.6	40.1	33.7	27.3	38.1	36.3

Table 1: Summary of the results on Nine domain-specific CL benchmarks with the Llama-2-7B. Averaged inference accuracy on the downstream tasks (Acc_t) is reported.

Downstream CL benchmarks for LLMs								
	C-STANCE	FOMC	MeetingBank	ScienceQA	NumGLUE-cm	20Minuten	MedMCQA	JEC-QA
Seq-Train	0	-10.0	-11.1	-13.4	-17.5	-26.0	-12.6	-16.1
ER	0	-7.0	-12.9	-15.2	-24.4	-26.2	-18.2	-14.8
EWC	0	-3.3	-10.2	-12.2	-20.6	-19.1	-19.4	-18.5
GEM	0	-3.7	-12.8	-13.6	-24.5	-21.8	-9.5	-17.6
A-GEM	0	-5.6	-13.0	-7.3	-22.0	-19.1	-12.4	-8.3
L2P	0	-9.0	-16.5	-11.8	-13.4	-21.4	-10.6	-8.6
PP	0	-2.4	-10.1	-9.7	-10.6	-10.8	-9.0	-14.2
I-LoRA	0	-0.6	-12.7	-6.1	-9.1	-15.2	-2.2	-2.3

Table 2: Summary of the results on Nine domain-specific CL benchmarks with the Llama-2-7B. Averaged memorization performance (BWT_t) is reported.

performance. From Table 1, we observe that: 1) starting from a fine-tuned LLaMA-7B language model, CL minima on different tasks can be connected by a low-loss valley, and ensembling over the valley shows improved performance and generalization ability. It is obvious that our approach, I-LoRA, consistently outperforms previous methods and shows a remarkable improvement (i.e., ranging from 3% to 10% accuracy gains) over the previous state-of-the-art CL methods. 2) I-LoRA consistently demonstrates superiority with an increasing number of historical tasks. This observation suggests that leveraging mode connectivity in LLMs could enhance long-term memorization ability and validate the effectiveness of long-term memory in I-LoRA.

Memorization Ability Assessment on Domain-specific CL benchmarks. In this part, we explore the memorization capability of continual learning (CL) methods, specifically examining the extent to which these methods can mitigate the issue of catastrophic forgetting. From Table 2, we can make the following observations: 1) I-LoRA exhibits superiority in mitigating forgetting issues and demon-

strates remarkable memorization ability. This observation validates our motivation and methodology design. I-LoRA adjusts parameters relying on the interpolation of mode connectivity, and its performance remains relatively stable throughout continual learning processes. 2) Existing CL-based methods exhibit weak performances when facing complex memorization tasks, such as those with high domain diversity and multilingualism. For example, one popular CL algorithm, EWC, shows a forgetting performance of 20.6% and 19.1% after fine-tuning on the mathematical NumGLUE-cm and German-based 20Minute dataset respectively. The diversity of sequential tasks makes these approaches ineffective. In contrast, our method achieves consistently promising performance, e.g., I-LoRA decreases the forgetting score to 9.1% on the NumGLUE-cm dataset. This boost in performance further validates our insight, which involves interpolating between adjacent minima and traversing along this path.

Fine-grained Analysis on Task-wise Performance To better understand how various methods achieve a balance between stability and plasticity,

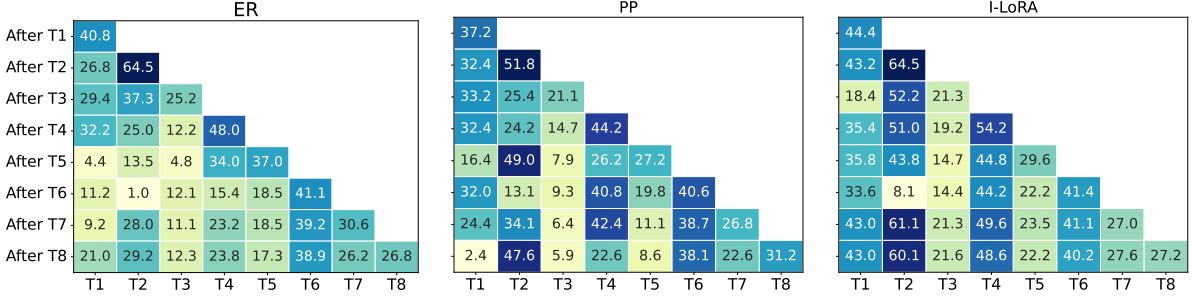


Figure 3: Task-wise performance of CL methods when Llama-2-7B is continually fine-tuned on the sequential tasks. The heatmaps provide the test set of each task (x-axis) evaluated at the end of each sequential learning task (y-axis).

we analyze how task-wise performance evolves as the model learns tasks sequentially. Experimental results are shown in Figure 3. The diagonal of the heatmap demonstrates the plasticity of the model as it denotes the learning of each new task. Due to the limit of space, we select two representative methods ER and PP as the baseline. The full experimental results are shown in Appendix.

Figure 3 demonstrates that the proposed I-LoRA offers a more consistent performance across the sequentially learned eight tasks compared to the baselines, showcasing a commendable balance between stability and plasticity. For example, the inference performance of ER on T3 dataset decreases from 12.2% to 4.8% at the endpoint of fine-tuning on T4 and T5, respectively. Similarly, the performance of PP drops from 14.7% to 7.9%. On the contrary, the proposed I-LoRA demonstrates a good trade-off between stability and plasticity, decreasing from 19.2% to 14.7%. After fine-tuning on T5, both ER and PP exhibit a much lower inference accuracy on previous tasks. For instance, ER achieves accuracy of 4.4%, 13.5%, and 4.8% on T1, T2, and T3, respectively. In contrast, I-LoRA demonstrates superior stability, achieving accuracy of 35.8%, 43.8%, and 14.7% on them.

Overall, I-LoRA provides an effective approach to leverage mode connectivity in continual fine-tuning of LLaMA-7B, enabling better utilization of long-term memory. This facilitates the effective consolidation of information across tasks and further mitigates forgetting.

Performance on General Tasks Evaluating the performance on general tasks is important in evaluating the memorization and reasoning abilities of Large Language Models (LLMs) after fine-tuning on domain-specific tasks. Table 3 displays the performance of continual learning (CL) methods, zero-shot inference performance of LLaMA-7B

Table 3: Performance on General Benchmarks after Fine-Tuning on Domain-Specific CL Benchmarks.

Method	MMLU	BBH	PIQA	GEN loss
Zero-Shot	46.8	38.2	78.3	—
Seq	3.68	28.82	58.49	-24.1
ER	5.22	28.67	53.1	-25.41
EWC	14.27	34.18	51.85	-21.0
GEM	15.45	31.74	53.48	-20.88
A-GEM	6.46	32.44	53.92	-23.49
L2P	2.24	31.95	54.19	-24.97
PP	30.58	16.97	53.05	-20.9
I-LoRA	15.77	32.66	51.25	-21.21
MTL	13.97	31.92	52.99	-21.47

(zero-shot), and multi-task learning method (MTL). Detailed evaluation metrics and dataset descriptions can be referred to Appendix. From these results, it can be observed that after continual learning processes, I-LoRA can still achieve an on-par performance with most baselines in these general language modeling tasks, despite a significant improvement in those specialized text domains as shown in Table 1 and 2. This phenomenon validates the advantage of I-LoRA in improving CL performance of LLMs.

5.3 Discussion

To further evaluate the effectiveness of I-LoRA in the continual refinement of LLaMA-7B, as discussed in Section 3, we examine how I-LoRA achieves a balance between plasticity and stability from three perspectives: 1) Weight Distance; 2) Centered Kernel Alignment; and 3) Mean Accuracy Landscape.

Weight Distance One intuitive explanation w.r.t the problem of catastrophic forgetting posits that after adapting to new data, LoRA parameters would change and converge toward another local optima,

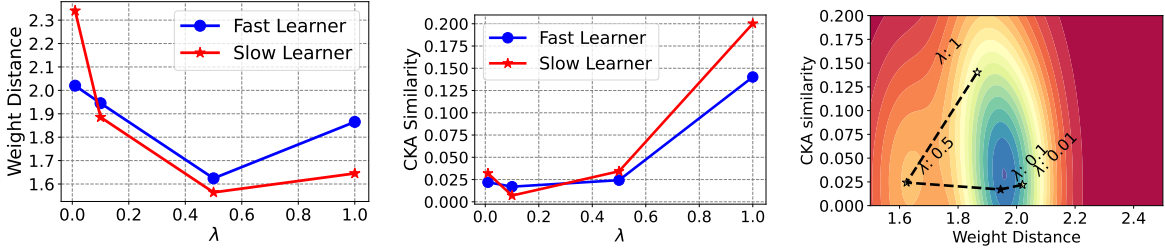


Figure 4: Task-wise performance of CL methods when Llama-2-7B is continually fine-tuned on the sequential tasks. The heatmaps provide the test set of each task (x-axis) evaluated at the end of each sequential learning task (y-axis).

which deviates from the historical one. Consequently, under the isotropic assumption of loss landscapes, the distance between historical and new weights can be used as a proxy for estimating the memorization of models. If parameters exhibit minimal change, it is rational to anticipate a lesser degree of forgetting. To this end, we propose to adopt the weight distance metric:

$$WD_l = \|\theta_t^l - \theta_{t+1}^l\|_2, \quad (7)$$

$$WD_w = \|\theta_t^w - \theta_{t+1}^w\|_2. \quad (8)$$

To evaluate the impact of weight interpolation, we measure the weight distance when varying λ to different values, and visualize the analysis results in Figure 4. When $\lambda = 0$, the effect of I-LoRA is similar to ER. Due to the constrained retention of memory samples, the current parameters of the fast learner, θ_{t+1}^s , may diverge significantly from its previous counterpart, θ_t^s , resulting in a substantial weight distance. Hence, as the value of λ increases, the current model weights tend to approach the previous weights more closely. However, the weight distance increases as λ is further raised. One plausible explanation is that the loss landscape becomes flatter in neighboring regions, and higher interpolation values may push the minima beyond these flat regions. Further analysis is provided in the Mean Accuracy Landscape Visualization section.

Centered Kernel Alignment In addition to considering weight distance, we further examine the produced representation space. To this end, we utilize Centered Kernel Alignment (CKA) (Kim et al., 2023; Mirzadeh et al., 2020) to assess the similarity of LoRA’s output representations. A higher similarity score indicates a greater stability and memorization ability of the continual minima.

The middle row of Figure 4 shows the CKA similarities with different interpolation ratios λ of the working memory and long-term memory. It is

obvious that the similarity in feature representation increases with a higher number of λ . Essentially, a higher λ indicates a slower update process based on historical LoRA parameters, which contributes to the stability of LLMs.

Embedding Landscape Visualization To illustrate the geometric characteristics of the landscape across different continual minima, as described in Figure 4, we depict the landscape of embedding changes after learning on task 1 and task 2 by perturbing LoRA parameters. Concretely, we vary the parameter on the subspace constructed by θ^w and θ^l , and visualize the extent of embedding change under different parameter interpolations.

As depicted in Figure 4, it’s evident that λ regulates the interpolation effects between continual minima and influences the convergence position on the loss landscape. A small value of *lambda* encourages adjacent minima to remain close, while an increasing value of *lambda* promotes slight changes in LoRA parameters and demonstrates high representation similarity. On the other hand, when the converged minima significantly diverges from the neighboring area of previous minima, LoRA will lose its capability in the trade-off.

6 Conclusion

Our empirical analysis provides comprehensive validation of the existence of intersections in loss landscapes surrounding task optima during Parameter-Efficient Fine-Tuning (PEFT) for LLMs. Building on this insight, we introduce I-LoRA, a pioneering approach that leverages two independent modules functioning as fast and slow learners, respectively. By promoting convergence between these modules and employing a linear interpolation, I-LoRA achieves a nuanced trade-off between plasticity and stability. As far as we are concerned, I-LoRA pioneers in enhancing CL for LLMs, and provide further opportunities for future explorations

7 Limitations

Although we believe that leveraging mode connectivity could potentially balance the trade-off between stability and plasticity, further theoretical analysis is warranted, and we have not yet explored this aspect in this study. In future research, we aim to develop a more comprehensive method that connects mode connectivity to continual fine-tuning for LLMs.

References

- Yonatan Bisk, Rowan Zellers, Ronan Le Bras, Jianfeng Gao, and Yejin Choi. 2019. [Piqa: Reasoning about physical commonsense in natural language](#).
- Pietro Buzzega, Matteo Boschini, Angelo Porrello, Davide Abati, and Simone Calderara. 2020. [Dark experience for general continual learning: a strong, simple baseline](#).
- Arslan Chaudhry, Marc’Aurelio Ranzato, Marcus Rohrbach, and Mohamed Elhoseiny. 2019a. [Efficient lifelong learning with a-GEM](#). In *International Conference on Learning Representations*.
- Arslan Chaudhry, Marcus Rohrbach, Mohamed Elhoseiny, Thalaisyasingam Ajanthan, Puneet K Dokania, Philip HS Torr, and Marc’Aurelio Ranzato. 2019b. On tiny episodic memories in continual learning. *arXiv preprint arXiv:1902.10486*.
- OpenCompass Contributors. 2023. Opencompass: A universal evaluation platform for foundation models. <https://github.com/open-compass/opencompass>.
- Thang Doan, Seyed Iman Mirzadeh, and Mehrdad Farajtabar. 2023. Continual learning beyond a single model. In *Conference on Lifelong Learning Agents*, pages 961–991. PMLR.
- Rahim Entezari, Hanie Sedghi, Olga Saukh, and Behnam Neyshabur. 2021. The role of permutation invariance in linear mode connectivity of neural networks. *arXiv preprint arXiv:2110.06296*.
- Jonathan Frankle, Gintare Karolina Dziugaite, Daniel Roy, and Michael Carbin. 2020. Linear mode connectivity and the lottery ticket hypothesis. In *International Conference on Machine Learning*, pages 3259–3269. PMLR.
- Qiankun Gao, Chen Zhao, Yifan Sun, Teng Xi, Gang Zhang, Bernard Ghanem, and Jian Zhang. 2023. A unified continual learning framework with general parameter-efficient tuning. *arXiv preprint arXiv:2303.10070*.
- Timur Garipov, Pavel Izmailov, Dmitrii Podoprikin, Dmitry P Vetrov, and Andrew G Wilson. 2018. Loss surfaces, mode connectivity, and fast ensembling of dnns. *Advances in neural information processing systems*, 31.
- Siavash Golkar, Michael Kagan, and Kyunghyun Cho. 2019. Continual learning via neural pruning. *Neurips*.
- Dan Hendrycks, Collin Burns, Steven Basart, Andy Zou, Mantas Mazeika, Dawn Song, and Jacob Steinhardt. 2021. [Measuring massive multitask language understanding](#).
- Edward J. Hu, Yelong Shen, Phillip Wallis, Zeyuan Allen-Zhu, Yuanzhi Li, Shean Wang, Lu Wang, and Weizhu Chen. 2021. [Lora: Low-rank adaptation of large language models](#).
- Yebowen Hu, Tim Ganter, Hanieh Deilamsalehy, Franck Dernoncourt, Hassan Foroosh, and Fei Liu. 2023. [Meetingbank: A benchmark dataset for meeting summarization](#).
- Haeyong Kang, Rusty John Lloyd Mina, Sultan Rizky Hikmawan Madjid, Jaehong Yoon, Mark Hasegawa-Johnson, Sung Ju Hwang, and Chang D Yoo. 2022. Forget-free continual learning with winning subnetworks. In *International Conference on Machine Learning*, pages 10734–10750. PMLR.
- Tannon Kew, Marek Kostrzewa, and Sarah Ebling. 2023. 20 minuten: A multi-task news summarisation dataset for german.
- Muhammad Gul Zain Ali Khan, Muhammad Ferjad Naeem, Luc Van Gool, Didier Stricker, Federico Tombari, and Muhammad Zeshan Afzal. 2023. Introducing language guidance in prompt-based continual learning. In *Proceedings of the IEEE/CVF International Conference on Computer Vision*, pages 11463–11473.
- Sanghwan Kim, Lorenzo Noci, Antonio Orvieto, and Thomas Hofmann. 2023. Achieving a better stability-plasticity trade-off via auxiliary networks in continual learning. In *Proceedings of the IEEE/CVF Conference on Computer Vision and Pattern Recognition*, pages 11930–11939.
- James Kirkpatrick, Razvan Pascanu, Neil Rabinowitz, Joel Veness, Guillaume Desjardins, Andrei A Rusu, Kieran Milan, John Quan, Tiago Ramalho, Agnieszka Grabska-Barwinska, et al. 2017. Overcoming catastrophic forgetting in neural networks. *Proceedings of the national academy of sciences*, 114(13):3521–3526.
- Timothée Lesort, Hugo Caselles-Dupré, Michael Garcia-Ortiz, Andrei Stoian, and David Filliat. 2019. Generative models from the perspective of continual learning. In *2019 International Joint Conference on Neural Networks (IJCNN)*, pages 1–8. IEEE.
- Zhizhong Li and Derek Hoiem. 2017. Learning without forgetting. *IEEE transactions on pattern analysis and machine intelligence*, 40(12):2935–2947.

- Pan Lu, Swaroop Mishra, Tony Xia, Liang Qiu, Kai-Wei Chang, Song-Chun Zhu, Oyvind Tafjord, Peter Clark, and Ashwin Kalyan. 2022. [Learn to explain: Multimodal reasoning via thought chains for science question answering](#).
- Seyed Iman Mirzadeh, Mehrdad Farajtabar, Dilan Gorur, Razvan Pascanu, and Hassan Ghasemzadeh. 2020. Linear mode connectivity in multitask and continual learning. *arXiv preprint arXiv:2010.04495*.
- Swaroop Mishra, Arindam Mitra, Neeraj Varshney, Bhavdeep Sachdeva, Peter Clark, Chitta Baral, and Ashwin Kalyan. 2022. Numglue: A suite of fundamental yet challenging mathematical reasoning tasks. *arXiv preprint arXiv:2204.05660*.
- Ankit Pal, Logesh Kumar Umapathi, and Malaikannan Sankarasubbu. 2022. [Medmcqa: A large-scale multi-subject multi-choice dataset for medical domain question answering](#). In *Proceedings of the Conference on Health, Inference, and Learning*, volume 174 of *Proceedings of Machine Learning Research*, pages 248–260. PMLR.
- Franco Pellegrini and Giulio Biroli. 2022. Neural network pruning denoises the features and makes local connectivity emerge in visual tasks. In *International Conference on Machine Learning*, pages 17601–17626. PMLR.
- Yujia Qin, Cheng Qian, Jing Yi, Weize Chen, Yankai Lin, Xu Han, Zhiyuan Liu, Maosong Sun, and Jie Zhou. 2022. Exploring mode connectivity for pre-trained language models. In *Proceedings of the 2022 Conference on Empirical Methods in Natural Language Processing*, pages 6726–6746.
- Anastasia Razdaibiedina, Yuning Mao, Rui Hou, Madihan Khabsa, Mike Lewis, and Amjad Almahairi. 2023. [Progressive prompts: Continual learning for language models](#). In *The Eleventh International Conference on Learning Representations*.
- David Rolnick, Arun Ahuja, Jonathan Schwarz, Timothy Lillicrap, and Gregory Wayne. 2019. Experience replay for continual learning. *Advances in Neural Information Processing Systems*, 32.
- Gobinda Saha, Isha Garg, and Kaushik Roy. 2021. Gradient projection memory for continual learning. *arXiv preprint arXiv:2103.09762*.
- Agam Shah, Suvan Paturi, and Sudheer Chava. 2023. [Trillion dollar words: A new financial dataset, task & market analysis](#). In *Proceedings of the 61st Annual Meeting of the Association for Computational Linguistics (Volume 1: Long Papers)*, pages 6664–6679, Toronto, Canada. Association for Computational Linguistics.
- Mirac Suzgun, Nathan Scales, Nathanael Schärli, Sebastian Gehrmann, Yi Tay, Hyung Won Chung, Aakanksha Chowdhery, Quoc V. Le, Ed H. Chi, Denny Zhou, and Jason Wei. 2022. [Challenging big-bench tasks and whether chain-of-thought can solve them](#).
- Liyuan Wang, Xingxing Zhang, Hang Su, and Jun Zhu. 2023a. A comprehensive survey of continual learning: Theory, method and application. *arXiv preprint arXiv:2302.00487*.
- Xiao Wang, Yuansen Zhang, Tianze Chen, Songyang Gao, Senjie Jin, Xianjun Yang, Zhiheng Xi, Rui Zheng, Yicheng Zou, Tao Gui, et al. 2023b. Trace: A comprehensive benchmark for continual learning in large language models. *arXiv preprint arXiv:2310.06762*.
- Zifeng Wang, Zizhao Zhang, Chen-Yu Lee, Han Zhang, Ruoxi Sun, Xiaoqi Ren, Guolong Su, Vincent Perot, Jennifer Dy, and Tomas Pfister. 2022. [Learning to prompt for continual learning](#).
- Haitao Wen, Haoyang Cheng, Heqian Qiu, Lanxiao Wang, Lili Pan, and Hongliang Li. 2023. Optimizing mode connectivity for class incremental learning. In *International Conference on Machine Learning*, pages 36940–36957. PMLR.
- Thomas Wolf, Lysandre Debut, Victor Sanh, Julien Chaumond, Clement Delangue, Anthony Moi, Pierric Cistac, Tim Rault, Rémi Louf, Morgan Funtowicz, Joe Davison, Sam Shleifer, Patrick von Platen, Clara Ma, Yacine Jernite, Julien Plu, Canwen Xu, Teven Le Scao, Sylvain Gugger, Mariama Drame, Quentin Lhoest, and Alexander M. Rush. 2020. [Transformers: State-of-the-art natural language processing](#). In *Proceedings of the 2020 Conference on Empirical Methods in Natural Language Processing: System Demonstrations*, pages 38–45, Online. Association for Computational Linguistics.
- Chenye Zhao, Yingjie Li, and Cornelia Caragea. 2023. C-stance: A large dataset for chinese zero-shot stance detection. In *Proceedings of the 61st Annual Meeting of the Association for Computational Linguistics (Volume 1: Long Papers)*, pages 13369–13385.
- Pu Zhao, Pin-Yu Chen, Payel Das, Karthikeyan Natesan Ramamurthy, and Xue Lin. 2020. Bridging mode connectivity in loss landscapes and adversarial robustness. *arXiv preprint arXiv:2005.00060*.
- Haoxi Zhong, Chaojun Xiao, Cunchao Tu, Tianyang Zhang, Zhiyuan Liu, and Maosong Sun. 2020. Jecqa: A legal-domain question answering dataset. In *Proceedings of AACL*.

A Detail Results of Performance in Domains Specific Benchmarks and General Benchmarks

We utilize OpenCompass (Contributors, 2023) with default settings to evaluate performance across three general benchmarks: MMLU (Hendrycks et al., 2021), BBH (Suzgun et al., 2022), and PIQA (Bisk et al., 2019). Some detailed results are shown in the following Tables.

Datasets	Prompts
C-STANCE	判断以下文本对指定对象的态度，选择一项：A.支持，B.反对，C.中立。输出A，B或者C。
FOMC	What is the monetary policy stance for the following text? A. dovish, B. hawkish, C. neutral. Choose one from A, B, and C.
MeetingBank	Write a summary of the following meeting transcripts.
ScienceQA	Choose an answer for the following question and give your reasons.
NumGLUE	Solve the following math problem.
20Minuten	Provide a simplified version of the following paragraph in German.
MedMCQA	Solve the following medical problem by choosing the correct answer from the following four choices.
JEC-QA	根据以下法律问题，从选项A，B，C，D中选择一项正确的答案

Table 4: Datasets’ Prompts

	C-STANCE	FOMC	MeetingBank	ScienceQA	NumGLUE-cm	20Minuten	MedMCQA	JEC-QA
C-STANCE	0.418	0.323	0.091	0.316	0.099	0.373	0.25	0.28
FOMC	0.218	0.603	0.091	0.216	0.049	0.37	0.226	0.256
MeetingBank	0.194	0.494	0.247	0.048	0.086	0.384	0.244	0.238
ScienceQA	0.32	0.262	0.148	0.368	0	0.367	0.226	0.238
NumGLUE-cm	0.256	0.204	0.057	0.244	0.333	0.37	0.162	0.252
20Minuten	0.002	0.012	0.087	0.158	0.148	0.414	0.222	0.144
MedMCQA	0.326	0.246	0.083	0.292	0.16	0.396	0.29	0.278
JEC-QA	0.164	0.258	0.093	0.096	0.123	0.39	0.26	0.296
Average	0.237	0.3	0.112	0.217	0.125	0.383	0.235	0.248
BWT	-0.184	AVE	0.21					

Table 5: LoRA adapter sequentially training

	C-STANCE	FOMC	MeetingBank	ScienceQA	NumGLUE-cm	20Minuten	MedMCQA	JEC-QA
C-STANCE	0.408	0.359	0.086	0.18	0.049	0.372	0.254	0.302
FOMC	0.268	0.645	0.073	0.09	0.037	0.371	0.238	0.238
MeetingBank	0.294	0.373	0.252	0.05	0.049	0.378	0.216	0.222
ScienceQA	0.322	0.25	0.122	0.48	0.025	0.375	0.202	0.274
NumGLUE-cm	0.044	0.135	0.048	0.34	0.37	0.377	0.206	0.244
20Minuten	0.112	0.01	0.121	0.154	0.185	0.411	0.234	0.226
MedMCQA	0.092	0.28	0.111	0.232	0.185	0.392	0.306	0.228
JEC-QA	0.21	0.292	0.123	0.238	0.173	0.389	0.262	0.268
Average	0.219	0.293	0.117	0.221	0.134	0.383	0.24	0.25
BWT	-0.169	AVE	0.244					

Table 6: ER replay with rate 0.1

	C-STANCE	FOMC	MeetingBank	ScienceQA	NumGLUE-cm	20Minuten	MedMCQA	JEC-QA
C-STANCE	0.422	0.488	0.061	0.08	0.086	0.372	0.238	0.248
FOMC	0.356	0.706	0.091	0.098	0.062	0.371	0.236	0.232
MeetingBank	0.338	0.484	0.256	0.082	0.049	0.374	0.24	0.208
ScienceQA	0.374	0.381	0.143	0.642	0.012	0.371	0.208	0.248
NumGLUE-cm	0.308	0.25	0.068	0.368	0.284	0.369	0.214	0.288
20Minuten	0.19	0.248	0.152	0.424	0.148	0.415	0.244	0.19
MedMCQA	0.194	0.349	0.086	0.142	0.198	0.401	0.276	0.142
JEC-QA	0.176	0.29	0.081	0.2	0.148	0.382	0.24	0.29
Average	0.295	0.4	0.117	0.255	0.123	0.382	0.237	0.231
BWT	-0.212	AVE	0.226					

Table 7: LoRA adapter training with EWC

	C-STANCE	FOMC	MeetingBank	ScienceQA	NumGLUE-cm	20Minuten	MedMCQA	JEC-QA
C-STANCE	0.388	0.29	0.104	0.364	0.062	0.373	0.244	0.268
FOMC	0.314	0.615	0.069	0.342	0.074	0.37	0.226	0.26
MeetingBank	0.174	0.444	0.233	0.182	0.049	0.383	0.228	0.22
ScienceQA	0.318	0.26	0.115	0.404	0.074	0.373	0.224	0.228
NumGLUE-cm	0.05	0.006	0.074	0.186	0.321	0.382	0.088	0.158
20Minuten	0.052	0.071	0.12	0.24	0.173	0.409	0.264	0.226
MedMCQA	0.32	0.262	0.077	0.47	0.185	0.389	0.292	0.25
JEC-QA	0.118	0.296	0.09	0.162	0.136	0.395	0.236	0.286
Average	0.217	0.281	0.11	0.294	0.134	0.384	0.225	0.237
BWT	-0.176	AVE	0.215					

Table 8: LoRA adapter training with GEM

	C-STANCE	FOMC	MeetingBank	ScienceQA	NumGLUE-cm	20Minuten	MedMCQA	JEC-QA
C-STANCE	0.402	0.28	0.075	0.374	0.062	0.374	0.254	0.286
FOMC	0.29	0.589	0.085	0.26	0.012	0.37	0.266	0.238
MeetingBank	0.118	0.484	0.24	0.222	0.074	0.38	0.226	0.146
ScienceQA	0.282	0.486	0.171	0.54	0.062	0.379	0.23	0.258
NumGLUE-cm	0.252	0.183	0.07	0.164	0.321	0.367	0.138	0.086
20Minuten	0.246	0.083	0.081	0.3	0.235	0.416	0.252	0.16
MedMCQA	0.192	0.462	0.06	0.334	0.21	0.379	0.278	0.216
JEC-QA	0.316	0.51	0.088	0.35	0.185	0.391	0.278	0.252
Average	0.262	0.385	0.109	0.318	0.145	0.382	0.24	0.205
BWT	-0.095	AVE	0.296					

Table 9: LoRA adapter training with A-GEM

	C-STANCE	FOMC	MeetingBank	ScienceQA	NumGLUE-cm	20Minuten	MedMCQA	JEC-QA
C-STANCE	0.438	0.258	0.115	0.42	0.062	0	0	0
FOMC	0.26	0.53	0.079	0.22	0.074	0.372	0.226	0.234
MeetingBank	0	0.472	0.248	0.022	0.025	0.374	0.176	0.152
ScienceQA	0.324	0.254	0.166	0.312	0.062	0.382	0.2	0.278
NumGLUE-cm	0.194	0.363	0.045	0.254	0.284	0.375	0.158	0.27
20Minuten	0	0.002	0.128	0.16	0.235	0.402	0.288	0.198
MedMCQA	0.002	0.264	0.143	0.408	0.259	0.393	0.258	0.262
JEC-QA	0.18	0.335	0.128	0.322	0.173	0.391	0.258	0.268
Average	0.175	0.31	0.132	0.265	0.147	0.336	0.196	0.208
BWT	-0.098	AVE	0.257					

Table 10: LoRA adapter training with Learning to Prompt

	C-STANCE	FOMC	MeetingBank	ScienceQA	NumGLUE-cm	20Minuten	MedMCQA	JEC-QA
C-STANCE	0.372	0.244	0.073	0.008	0.012	0.374	0.08	0.108
FOMC	0.324	0.518	0.057	0.02	0.025	0.373	0.158	0.236
MeetingBank	0.332	0.254	0.211	0.032	0	0.374	0.212	0.048
ScienceQA	0.324	0.242	0.147	0.422	0.025	0.377	0.23	0.248
NumGLUE-cm	0.164	0.49	0.079	0.262	0.272	0.378	0.172	0.18
20Minuten	0.32	0.131	0.093	0.408	0.198	0.406	0.218	0.254
MedMCQA	0.244	0.341	0.064	0.424	0.111	0.387	0.268	0.224
JEC-QA	0.024	0.476	0.059	0.226	0.086	0.381	0.226	0.312
Average	0.263	0.337	0.098	0.225	0.091	0.381	0.196	0.201
BWT	-0.142	AVE	0.224					

Table 11: LoRA training with Progerssize Prompts

C-STANCE	FOMC	MeetingBank	ScienceQA	NumGLUE-cm	20Minuten	MedMCQA	JEC-QA
0.384	0.506	0.252	0.586	0.284	0.416	0.248	0.244

Table 12: Multi task training

C-STANCE	FOMC	MeetingBank	ScienceQA	NumGLUE-cm	20Minuten	MedMCQA	JEC-QA
0.35	0.24	0.10	0.23	0.28	0.30	0.24	0.12

Table 13: zero-shot inference results

	C-STANCE	FOMC	MeetingBank	ScienceQA	NumGLUE-cm	20Minuten	MedMCQA	JEC-QA
C-STANCE	0.388	0.276	0.081	0.426	0.049	0.377	0.226	0.278
FOMC	0.342	0.488	0.101	0.074	0.049	0.373	0.23	0.202
MeetingBank	0.164	0.032	0.233	0.002	0.037	0.388	0.222	0.194
ScienceQA	0.324	0.252	0.099	0.434	0.012	0.382	0.196	0.282
NumGLUE-cm	0.308	0.004	0.059	0.31	0.148	0.375	0.2	0.25
20Minuten	0.014	0.014	0.063	0.032	0.062	0.412	0.07	0.018
MedMCQA	0.328	0.236	0.057	0.062	0.111	0.373	0.258	0.274
JEC-QA	0.324	0.272	0.068	0.222	0.049	0.381	0.25	0.284

Table 14: Single task fine-tuning

Table 15: Linear combination with learning fast and slow

	C-STANCE	FOMC	MeetingBank	ScienceQA	NumGLUE-cm	20Minuten	MedMCQA	JEC-QA
C-STANCE	0.444	0.357	0.066	0.122	0.111	0.374	0.254	0.292
FOMC	0.432	0.645	0.066	0.1	0.074	0.37	0.236	0.266
MeetingBank	0.184	0.522	0.213	0.26	0.074	0.384	0.244	0.236
ScienceQA	0.354	0.51	0.192	0.542	0.025	0.378	0.214	0.226
NumGLUE-cm	0.358	0.438	0.147	0.448	0.296	0.383	0.196	0.268
20Minuten	0.336	0.081	0.144	0.442	0.222	0.414	0.244	0.206
MedMCQA	0.43	0.611	0.213	0.496	0.235	0.411	0.27	0.29
JEC-QA	0.43	0.601	0.216	0.486	0.222	0.402	0.276	0.272
Average	0.371	0.471	0.157	0.362	0.157	0.39	0.242	0.257
BWT	-0.027	AVE	0.363					

Table 16: Detailed Results of General Benchmarks

dataset	version	metric	mode	SEQ	EWC	ER	GEM	AGEM	L2P	PP	MTL	OURS
lukaemon_mmlu_college_biology	8c2e29	accuracy	gen	0.69	20.83	0.69	14.58	2.78	3.47	33.33	21.53	0
lukaemon_mmlu_college_chemistry	0afccd	accuracy	gen	2	12	3	7	3	1	13	13	3
lukaemon_mmlu_college_computer_science	c1c1b4	accuracy	gen	5	16	7	18	9	3	22	8	4
lukaemon_mmlu_college_mathematics	9deed0	accuracy	gen	8	23	11	7	2	0	13	18	4
lukaemon_mmlu_college_physics	f5cf5e	accuracy	gen	0	8.82	0	2.94	0	0.98	3.92	15.69	0
lukaemon_mmlu_electrical_engineering	3d694d	accuracy	gen	0	13.79	8.28	6.21	1.38	1.38	31.03	20	1.38
lukaemon_mmlu_astronomy	7ef16f	accuracy	gen	4.61	12.5	1.97	33.55	1.32	0	26.97	16.45	6.58
lukaemon_mmlu_anatomy	2d597d	accuracy	gen	1.48	17.04	0	9.63	5.93	0	37.04	5.93	5.19
lukaemon_mmlu_abstract_algebra	ec092c	accuracy	gen	7	25	8	15	2	3	22	23	12
lukaemon_mmlu_machine_learning	d489ae	accuracy	gen	17.86	25	14.29	3.57	0	0.89	20.54	4.46	0
lukaemon_mmlu_clinical_knowledge	af10df	accuracy	gen	0.75	26.42	1.89	8.68	0.75	0	34.34	10.19	1.51
lukaemon_mmlu_global_facts	cad9e0	accuracy	gen	1	29	10	30	3	0	22	28	5
lukaemon_mmlu_management	65f310	accuracy	gen	0	25.24	1.94	24.27	0	0	30.1	14.56	0
lukaemon_mmlu_nutrition	80bf96	accuracy	gen	0	19.61	2.29	15.36	7.19	0.65	32.03	8.82	11.11
lukaemon_mmlu_marketing	9a98c0	accuracy	gen	0.43	25.64	2.56	5.13	11.54	21.37	50.85	7.26	0.43
lukaemon_mmlu_professional_accounting	9cc7e2	accuracy	gen	5.32	20.21	15.96	21.99	12.06	13.83	20.92	20.92	13.83
lukaemon_mmlu_high_school_geography	c28a4c	accuracy	gen	0.51	21.72	0.51	5.56	1.52	0	33.84	2.53	5.56
lukaemon_mmlu_international_law	408d4e	accuracy	gen	32.23	24.79	1.65	52.07	47.93	1.65	47.93	45.45	0
lukaemon_mmlu_moral_scenarios	9f30a6	accuracy	gen	0	24.25	0.11	19.33	24.25	0	24.13	24.25	0.22
lukaemon_mmlu_computer_security	2753c1	accuracy	gen	1	18	2	4	0	0	44	17	0
lukaemon_mmlu_high_school_microeconomics	af9eae	accuracy	gen	0.42	22.69	0	21.85	12.18	0.42	27.73	9.24	13.87
lukaemon_mmlu_professional_law	7c7a62	accuracy	gen	6.06	18.9	3.65	29.14	16.36	0.52	29.14	21.71	3.13
lukaemon_mmlu_medical_genetics	b1a3a7	accuracy	gen	0	19	5	3	1	1	35	5	0
lukaemon_mmlu_professional_psychology	c6b790	accuracy	gen	0.98	14.38	1.31	22.88	11.44	0.16	39.22	13.24	0.98
lukaemon_mmlu_jurisprudence	f41074	accuracy	gen	0	28.7	0	29.63	0.93	0	43.52	25	0
lukaemon_mmlu_world_religions	d44a95	accuracy	gen	0.58	20.47	4.68	41.52	5.85	4.09	47.37	2.92	1.17
lukaemon_mmlu_philosophy	d36ef3	accuracy	gen	1.61	27.01	3.54	4.5	11.9	1.61	37.94	7.4	0.96
lukaemon_mmlu_virology	0a5f8e	accuracy	gen	0	29.52	9.04	3.01	0.6	0	33.13	16.87	2.41
lukaemon_mmlu_high_school_chemistry	5b2ef9	accuracy	gen	2.46	15.76	2.46	10.84	3.45	1.48	29.06	14.29	2.46
lukaemon_mmlu_public_relations	4c7898	accuracy	gen	0.91	31.82	11.82	4.55	0.91	0	32.73	20	0
lukaemon_mmlu_high_school_macro_economics	3f841b	accuracy	gen	4.87	19.74	8.46	13.08	2.56	0	22.56	7.95	7.18
lukaemon_mmlu_human_sexuality	4d1f3e	accuracy	gen	0.76	15.27	4.58	2.29	2.29	0	35.88	4.58	0.76
lukaemon_mmlu_elementary_mathematics	0f5d3a	accuracy	gen	1.32	14.29	5.03	21.96	3.44	2.12	18.25	12.96	7.14
lukaemon_mmlu_high_school_physics	0dd929	accuracy	gen	5.96	12.58	1.99	13.25	3.97	2.65	20.53	15.89	8.61
lukaemon_mmlu_high_school_computer_science	bf31fd	accuracy	gen	5	23	8	17	4	1	30	18	3
lukaemon_mmlu_high_school_european_history	d1b67e	accuracy	gen	16.97	23.03	12.12	21.21	15.76	11.52	26.67	9.7	6.06
lukaemon_mmlu_business_ethics	af53f3	accuracy	gen	0	26	0	5	1	1	39	15	0
lukaemon_mmlu_moral_disputes	48239e	accuracy	gen	0	24.86	0.58	24.57	4.05	8.09	37.28	5.78	9.54
lukaemon_mmlu_high_school_statistics	47e18e	accuracy	gen	4.63	14.81	8.8	18.52	5.09	2.78	15.74	3.7	7.87
lukaemon_mmlu_miscellaneous	573569	accuracy	gen	1.4	27.71	19.67	23.5	5.49	0.51	44.7	24.14	7.41
lukaemon_mmlu_formal_logic	7a0414	accuracy	gen	2.38	18.25	7.14	17.46	15.87	1.59	19.84	10.32	6.35
lukaemon_mmlu_high_school_government_and_politics	d907eb	accuracy	gen	0	20.73	0.52	30.57	2.59	0	36.27	22.28	17.62
lukaemon_mmlu_prehistory	65aa94	accuracy	gen	3.4	23.15	4.01	18.83	4.32	1.23	36.73	21.3	1.85
lukaemon_mmlu_security_studies	9ea7d3	accuracy	gen	0.41	15.92	2.04	26.53	6.53	3.27	26.53	16.73	3.67
lukaemon_mmlu_high_school_biology	775183	accuracy	gen	0.65	25.16	0.65	9.03	3.23	0.97	37.1	1.94	14.19
lukaemon_mmlu_logical_fallacies	19746a	accuracy	gen	1.84	24.54	6.75	12.88	12.88	0.61	31.9	11.04	6.13
lukaemon_mmlu_high_school_world_history	6665dc	accuracy	gen	18.57	26.58	10.13	7.59	23.63	23.21	21.1	9.7	8.44
lukaemon_mmlu_professional_medicine	a05bab	accuracy	gen	9.93	15.07	4.04	8.09	1.1	0	38.97	1.1	5.51
lukaemon_mmlu_high_school_mathematics	0e6a7e	accuracy	gen	4.81	16.3	5.56	22.59	3.33	0.37	18.89	13.7	3.33
lukaemon_mmlu_college_medicine	5215f1	accuracy	gen	1.16	14.45	2.31	5.78	1.16	1.73	28.9	9.25	2.31
lukaemon_mmlu_high_school_us_history	b5f235	accuracy	gen	8.82	18.63	1.47	20.1	11.76	2.94	18.63	9.31	2.94
lukaemon_mmlu_sociology	4980ec	accuracy	gen	3.98	21.89	8.96	4.48	5.97	0	41.79	6.47	2.49
lukaemon_mmlu_econometrics	4d590b	accuracy	gen	7.02	24.56	2.63	16.67	12.28	0.88	25.44	9.65	0.88
lukaemon_mmlu_high_school_psychology	440e98	accuracy	gen	0.73	22.57	0.55	10.28	8.99	0.73	37.61	9.72	12.48
lukaemon_mmlu_human_aging	d0a8e1	accuracy	gen	0.9	36.77	15.25	0.45	0.9	0	39.01	23.32	4.93
lukaemon_mmlu_us_foreign_policy	adcc88	accuracy	gen	1	21	13	22	5	0	44	14	20
lukaemon_mmlu_conceptual_physics	a111d3	accuracy	gen	0	22.13	8.51	11.91	0.85	0	31.91	28.09	2.55

Table 17: Detailed Results of General Benchmarks

dataset	version	metric	mode	SEQ	EWC	ER	GEM	AGEM	L2P	PP	MTL	OURS
bbh-temporal_sequences	e43931	score	gen	8.4	16.4	19.2	17.2	18.4	22.4	24.4	19.6	15.2
bbh-disambiguation_qa	d52c61	score	gen	30	30.8	31.2	29.6	30	30	30	34.8	30.8
bbh-date_understanding	a8000b	score	gen	32	26	27.6	36.8	32	39.2	33.2	38	27.6
bbh-tracking_shuffled_objects_three_objects	7964c0	score	gen	32.8	34.4	29.2	28.4	33.2	31.6	29.2	35.2	32.8
bbh-penguins_in_a_table	fceb27	score	gen	32.88	29.45	28.08	26.03	35.62	35.62	30.14	32.88	30.82
bbh-geometric_shapes	503c8f	score	gen	4.8	8.8	0.4	0.8	0	0	3.2	2	3.2
bbh-snarks	42d6ca	score	gen	46.07	50	47.75	54.49	53.37	50.56	51.12	50	48.31
bbh-ruin_names	408de8	score	gen	23.2	27.2	24.4	24.8	22.4	24.4	22.4	29.2	24
bbh-tracking_shuffled_objects_seven_objects	7964c0	score	gen	17.6	19.6	16	16	17.6	13.6	17.2	12.4	15.6
bbh-tracking_shuffled_objects_five_objects	7964c0	score	gen	16.8	17.6	14	16	20.8	13.2	17.2	14.4	18.4
bbh-logical_deduction_three_objects	45ebc5	score	gen	35.6	32.4	42	44	50.4	45.6	42	41.2	39.6
bbh-hyperbaton	5e5016	score	gen	53.2	55.2	54.8	53.6	55.6	56.8	53.6	53.2	48.8
bbh-logical_deduction_five_objects	45ebc5	score	gen	22.8	17.2	19.6	21.2	28.8	23.2	23.2	22.8	27.6
bbh-logical_deduction_seven_objects	45ebc5	score	gen	14.4	12.4	10.4	19.2	20.4	19.2	19.6	13.6	13.2
bbh-movie_recommendation	cc2fde	score	gen	31.2	41.2	36.4	62.4	60.8	63.6	62.4	53.6	34
bbh-salient_translation_error_detection	5b5f35	score	gen	10.8	11.6	13.6	14	18	11.2	12	18.8	6.4
bbh-reasoning_about_colored_objects	1cb761	score	gen	21.6	16.8	18.4	22.4	25.2	26	24.4	22.8	21.6
bbh-multistep_arithmetic_two	30f91e	score	gen	0	0	1.2	0.4	0.4	1.2	0.4	1.6	1.2
bbh-navigate	1576d9	score	gen	40.8	43.2	51.6	45.6	46.8	48.8	48	54.8	46
bbh-dyck_languages	805bea	score	gen	0	0.4	0	0.4	0	0	0.8	0	0.4
bbh-word_sorting	9a3f78	score	gen	3.2	1.2	1.6	5.2	4.8	4.8	6.4	6.8	2.8
bbh-sports_understanding	d3fa77	score	gen	87.2	79.2	90.8	88	78.8	84	84	77.6	90.8
bbh-boolean_expressions	612c92	score	gen	61.6	47.2	65.2	62.8	63.6	60.4	55.6	61.2	63.6
bbh-object_counting	781e5c	score	gen	47.6	50.8	41.6	45.6	50	50.4	56	48	43.2
bbh-formal_fallacies	eada96	score	gen	15.6	12.8	2.8	26.8	24	19.6	27.2	13.6	2.4
bbh-causal_judgement	89eaa4	score	gen	36.9	34.76	37.43	41.71	35.83	39.57	44.92	50.27	33.16
bbh-web_of_lies	0c0441	score	gen	51.2	42.8	51.2	53.6	49.2	47.6	53.6	53.6	52.4
piqa	1194eb	accuracy	gen	58.49	47.12	53.1	53.48	53.92	54.19	53.05	52.99	51.25